Journal of
Biomaterials and Tissue Engineering
Vol. 4, 379–388, 2014

RESEARCH ARTICLE

Structural and Biological Comparison of Cryopreserved and Fresh Amniotic Membrane Tissues

Ek Kia Tan[1,2], Marissa Cooke[3], Christian Mandrycky[3], Megha Mahabole[1,2], Hua He[1,2], Julie O'Connell[4], Todd C. McDevitt[3,5], and Scheffer C. G. Tseng[1,2,*]

[1] *TissueTech, Inc., Miami, 33173, Florida, USA*
[2] *Ocular Surface Center, Miami, 33173, Florida, USA*
[3] *Wallace H. Coulter Department of Biomedical Engineering at Georgia Institute of Technology and Emory University, Atlanta, GA, 30332-0535, USA*
[4] *Amniox Medical, Atlanta, GA, 30339, USA*
[5] *Parker H. Petit Institute for Bioengineering and Bioscience, Georgia Institute of Technology, Atlanta, GA, 30339, USA*

The use of amniotic membrane (AM) to modulate wound healing and promote regeneration is increasing, but to date there has been no comprehensive study directly comparing the structural and biological properties of fresh and cryopreserved AM. Thus, in this study we compared fresh AM and fresh amniochorion to cryopreserved tissues. Histochemical staining confirmed that the cryopreservation process did not dramatically alter the tissue architecture nor collagen and glycosaminoglycan density. Biochemically, cryopreservation reduced total protein and human serum albumin contents, but retained high molecular weight hyaluronic acid species including the heavy chain-hyaluronic acid complex that is known to exert anti-inflammatory and anti-scarring effects. Cryopreserved and fresh AM extracts similarly suppressed viability and proliferation of RAW264.7 macrophages, and inhibited the transforming growth factor beta 1 promoter activity in corneal fibroblasts. These results collectively indicate that cryopreservation effectively preserves histological, biochemical, and functional properties of the AM tissue.

Keywords: Amniotic Membrane, Cryopreserved, Fresh, Histology, Anti-Inflammatory, Anti-Scarring.

1. INTRODUCTION

Amniotic membrane (AM) shares the same cell origin as the fetus and comprises the inner most layer of the placenta that enwraps and protects the fetus during development from unwanted maternal immunological insults.[1] As a result, the tissue inherently contains a number of biological modulators to combat inflammation.[2] Although the first reported clinical application of AM was for skin transplantation in 1910,[3] it was not until the late 20th century when clinical use of AM in ocular surface indications soared and its use in open wounds,[4,5] skin burns[6,7] and leg ulcers grew in popularity.[8,9] To date, more than 1000 peer reviewed papers have been published (Pubmed keyword search for "amniotic membrane transplantation") examining the therapeutic potential of AM in a variety of clinical indications, particularly in ophthalmology.[1,2,10–12] These studies have demonstrated the ability of AM to promote adult wound healing towards regeneration with minimal inflammation and scarring, similar to fetal tissues.[13,14] In ophthalmology, cryopreserved AM has been used as a permanent graft to fill in tissue defects and to allow the integration of host cells, or as a temporary biological bandage to facilitate wound healing by suppressing excessive surgical or disease-induced host tissue inflammation.[2] Additionally, the clinical success of AM as a potent anti-inflammatory and anti-scarring agent has prompted numerous investigations into its use for various orthopedic applications to decrease local inflammation and adhesion formation following tendon[15,16] and nerve repair.[17–19]

As with many allografts, the use of fresh tissue is often impractical and can pose a serious risk of disease transmission,[20,21] therefore processing methods must be used. In this case, effective tissue preservation and storage are essential for maintaining the therapeutic actions of the fresh material and are critical to the successful commercialization of AM tissues for clinical use. While multiple

*Author to whom correspondence should be addressed.

AM preservation methods exist (including dehydration, lyophilization, chemical cross-linking, and cryopreservation), these processing methods all have variable effects on preserving the native form of AM tissue, and can dramatically alter the type of host response elicited to the material when utilized as templates for tissue regeneration.[22] Ideally, tissue processing methods should preserve both the structural integrity and biomechanical stability of the tissue, as well as the activity of critical cell signaling factors (i.e., cytokines, growth factors and proteoglycans) contained within the matrix that are essential for its intended clinical use.

The primary objective of this study was to examine the effect cryopreservation has on both AM matrix structural integrity and the retention of key signaling factors and biological activities necessary for the therapeutic efficacy of the tissue. The structural components of cryopreserved and fresh AM tissues were analyzed using histology and histochemistry while their protein composition were elucidated by Western blot and ELISA. Additionally, macrophage and fibroblast functional assays were utilized to examine the effect of cryopreservation on the anti-inflammatory activity of AM tissues by comparing cryopreserved and fresh AM tissue extracts.

2. MATERIALS AND METHODS

2.1. Materials

Guanidine hydrochloride, anhydrous alcohol, bovine serum albumin (BSA), Hoechst 33342, sodium chloride, sodium hydroxide, Tris base, and Triton X-100, were obtained from Sigma-Aldrich (St. Louis, MO). *Streptomyces hyalurolyticus* hyaluronidase (HAase) and biotinylated Hyaluronic Acid Binding Protein (HABP) were from Seikagaku Biobusiness Corporation (Tokyo, Japan). Dulbecco's modified Eagle's medium (DMEM), fetal bovine serum (FBS), Hank's balanced salt solution, gentamicin, amphotericin B, agarose, phosphate buffered saline (PBS), LIVE/DEAD Cell Viability Assay, and Alexa Fluor® 488 streptavidin were purchased from Invitrogen (Grand Island, NY). Select-HA HiLadder (molecular mass of 1510, 1090, 966, 572, and 495 kDa) was from AMS Biotechnology, UK. A medical grade high molecular weight (HMW) hyaluronic acid (HA), Healon® (∼4000 kDa), was from Advanced Medical Optics (Santa Ana, CA). CellBIND® 24-well plate (3337) and 96-well plate (3596) were from Corning (Lowell, MA). Bicinchoninic Acid (BCA) Protein Assay Kit (23225) was from Pierce (Rockford, IL). HA Quantitative Test Kit (029-001) was from Corgenix (Westminster, CO). Human Serum Albumin EIA Kit was from Cayman Chemicals (Ann Arbor, MI). Laemmli Buffer (161-0737), 4–15% gradient acrylamide ready gels (161-1176), 10x Tris/Glycine/SDS Buffer (161-0732), and 0.45 μm nitrocellulose membranes (162-0145) were from Bio-Rad (Hercules, CA). Cell proliferation Bromodeoxyuridine (BrdU) ELISA (11647229001) was from Roche (Mannheim, Germany). IαI were prepared from human plasma according to published methods.[23,24] RAW264.7 cells were from ATCC (Manassas, VA). Mouse anti-human ITIH1 polycolonal antibody (HC1) against full length ITIH1 was purchased from Abcam Inc. (Cambridge, MA). Western Lighting™ Chemiluminesence Reagent was from PerkinElmer, Inc. (Waltham, MA). Antibody diluent, rabbit anti-mouse HRP-conjugated antibody, and diaminobenzidine were from Dako Cytomation (Carpentaria, CA). Slide-A-Lyzer Dialysis Cassettes (3.5 K MWCO) and Wheaton Dounce Tissue Grinder were from Fisher Scientific (Pittsburgh, PA). BioPulverizer was from Biospec Products, Inc. (Bartlesville, OK).

2.2. Tissue Preparation

Cryopreserved human AM tissue processed by the CryoTek™ (CT) method was kindly provided by TissueTech™ (Miami, FL). Donated full term human placenta after cesarean section delivery was recovered in compliance with American Association of Tissue Banks (AATB) Standards and immediately stored at − 80 °C for up to 1 year. Prior to processing, the frozen placenta was thawed at room temperature for 8 h in a Good Manufacturing Practice (GMP) facility before being placed at 8 °C for an additional 16 h. Under aseptic conditions, the placenta was first cleaned of blood clots with PBS prior to separation of AM by blunt dissection. The AM was gently rinsed in PBS until all blood coloration was removed before being affixed on a filter membrane and cut to 3×6 cm. The AM tissue was finally packaged in a pouch containing 1:1 Dulbecco Modified Eagle Medium (DMEM) and glycerol before storage at − 80 °C for up to 2 years or until required. Fresh full-term human placenta was procured within 6 hour of delivery from a healthy mother, with donor consent after elective caesarean delivery in Baptist Hospital (Miami, FL) via an approved protocol (Protocol 03-028) by the Baptist Health South Florida Institutional Review. The fresh placenta was immediately processed by removing blood clots with PBS prior to separation of AM with blunt dissection. The fresh AM was then affixed on a filter membrane and cut to 3×6 cm. The fresh AM tissue was kept in a sterile dish containing PBS at 4 °C and used within 24 h of processing. Six different types of tissues were prepared: fresh AM (F-Thin, F-Thick), cryopreserved AM (CT-Thin, CT-Thick), and fresh and cryopreserved amniochorion (F-AMC and CT-AMC, respectively). The blunt dissection step to separate chorion was omitted to prepare AMC tissue.

2.3. Histology, Histochemical Staining, and Histochemistry

Cryopreserved tissues were allowed to thaw for 10 min at room temperature. Fresh and cryopreserved tissues were fixed with 10% formalin for 1 h, washed three times with

PBS for 5 min each, and cut with a 15-mm biopsy punch to obtain equal-sized tissue samples. Tissues were subsequently embedded in histogel, processed, embedded into paraffin blocks, and cut into 5 μm sections. Histological sections were then stained with either hematoxylin and eosin (H&E), Masson's trichrome (MAS), or Safranin O (SafO) with Fast Green FCF counterstain. For HA histochemistry, de-paraffinized sections were pretreated with or without HAase for 2 h at 37 °C in a wet chamber and permeabilized with a 0.2% Triton X-100 solution in PBS for 30 min. After three rinses with PBS for 5 min each and pre-incubation with 2% BSA in PBS to block non-specific staining for 30 min, sections were incubated with biotinylated HABP (1:100) in antibody diluent for 16 h at 4 °C. After three more rinses with PBS for 5 min each, the sections were incubated with Alexa Fluor® 488 streptavidin (1:100) in antibody diluent for 1 h. Nuclei were counterstained with Hoechst 33342 (1:500) in PBS for 1 min before the sections were rinsed three times with PBS for 5 min each. Images were photographed by laser confocal microscopy (LSM700 on Axio Observer.Z1, Zeiss).

2.4. Tissue Extract Preparation

The preparation of AM extract (AME) from AM tissue was carried out aseptically as previously reported.[25] AM tissue with a size of approximately 6 × 6 cm was rinsed with PBS and placed in a BioPulverizer before being snap-frozen in liquid nitrogen and pulverized for 10 cycles. Each pulverization cycle comprised of hammering the pestle into the mortar containing the frozen tissue 3 times. Pulverized tissue fragments were resuspended in PBS at a 1:3 (W/V) ratio before homogenization with Wheaton Dounce for another 10 cycles. Each homogenization cycle comprised of injecting the pestle into the end of the mortar containing liquefied tissue fragments. To assess the retention of key biochemical molecules, homogenized tissues were extracted by 4M guanidine hydrochloride at a 1:6 (W/V) ratio for 16 h at 4 °C with a reagent rotator (Multi-Mix, VWR) before centrifugation at 48,000× g for 30 min at 4 °C (Avanti J-20I, Beckman Coulter). The supernatant was then dialyzed against PBS for 30 h with Slide-A-Lyzer (3.5 K MWCO) to obtain water-soluble extracts from each tissue. Protein content was quantified using a standard BCA assay while quantification of human serum albumin and HA was performed by ELISA and HABP-coated microwell kit, respectively.

2.5. Determination of HA Sizes by Agarose Gel Electrophoresis

The molecular weight of HA in AME was analyzed by agarose gel electrophoresis as previously reported.[26] AME was loaded at the same equivalent (15 μg) of HA per lane with or without 9 units of HAase pre-treatment at 37 °C for 1 h, then separated on a 0.5% agarose gel at 20 V for the first 30 min and 40 V for 4 h thereafter. The gel was subsequently stained with 0.005% Stains-all dye in 50% ethanol overnight at 25 °C in the dark before de-staining in water and exposing to ambient light for 6 h. The molecular weight range of HA samples, which appear as a bluish smear on the agarose gel, were estimated by comparison to the Select-HA HiLadder and HMW HA (Healon®).

2.6. Western Blot

AME samples were loaded with 20 μg protein per lane with or without 2 units of HAase pre-treatment at 37 °C for 1 h before denaturation in Laemmli Buffer (1:1 dilution with sample) at 95 °C for 5 min. Samples were electrophoresed on a 4–15% (w/v) gradient acrylamide ready gel in 1× Tris/Glycine/SDS Buffer at 150 V for approximately 1 h and electrophoretically transferred to a 0.45 μm nitrocellulose membrane. The membrane was then blocked with 5% fat-free milk in TBST (50 mM Tris-HCl, pH 7.5, 150 mM NaCl, 0.05% Tween 20) and sequentially incubated with mouse anti-human primary antibodies against HC1 (1:1000) in 5% fat-free milk in TBST for 16 h at 4 °C with a rotator (Maxi Rotator, Labline). After three rinses in TBST for 10 minutes each, the nitrocellulose membrane was incubated with rabbit anti-mouse HRP-conjugated secondary antibody (1:1000) in 5% fat-free milk in TBST for 2 h at room temperature with an orbital shaker (MaxQ 2500, Thermo Scientific) followed by three rinses in TBST for 10 min each. Immunoreactive protein bands were detected with Western Lighting™ Chemiluminesence Reagent and imaged by a Luminescent Image Analyzer (ImageQuant™ LAS 4000, GE).

2.7. Macrophage Viability and Proliferation Assay

Due to the inability to image the thick tissues, only the thin tissue was used for the functional analysis. F-Thin and CT-Thin AM tissue with a size of approximately 2.5 × 2.5 cm were fastened on 15 mm culture inserts with the stromal tissue side facing up as previously described.[27] For the macrophage viability assay, RAW264.7 cells were seeded at a density of 113 cells/mm^2 in DMEM/10% FBS and cultured for 48 h. After two rinses with PBS, a LIVE/DEAD assay was used to determine cell viability under a fluorescent microscope (TE-2000U, Nikon). For the macrophage proliferation assay, RAW264.7 cells were seeded at a density of 95 cells/mm^2 on plastic 96-well plate in DMEM/10% FBS and treated simultaneously with 100 μg/ml AME derived from either F-Thin or CT-Thin, as well as a PBS vehicle control (CTL). After 48 hours, the RAW264.7 cells were labeled with 10 μM BrdU for 1 h. Subsequently, the RAW264.7 cells were fixed with FixDenat (provided in BrdU ELISA kit) at 25 °C for 30 min, followed by incubation with anti-BrdU-peroxidase conjugated at 25 °C for 2 h. The color was developed for 30 min by adding the substrate TMB (tetramethyl-benzidine) and

quenched by adding 1 M H_2SO_4. Colorimetric measurements were performed at 450 nm with a reference wavelength at 690 nm.

2.8. Transforming Growth Factor Beta 1 (TGF-β1) Promoter Assay

Expression of the TGF-β1 gene was measured by a promoter assay in human corneal fibroblasts cultured to 80% confluence in DMEM/10% FBS as previously reported.[28] After washing the cultures twice with the medium listed above, the cells were treated with adeno-TGF-β1 promoter luciferase (multiplicity of infection = 37.5) and adeno-CMV-β-galactosidase (multiplicity of infection = 30), and incubated at 37 °C for 4 h before being harvested and reseeded at 95 cells/mm^2 on plastic 96-well plates. After 2 h, AME at a series of protein concentration ranging from 0.008–125 μg/ml obtained from F-Thin or CT-Thin as well as a PBS vehicle control (CTL) were added to the culture medium and cells were incubated for an additional 42 h, for a combined total of 48 h transfection. The culture medium was then removed and cells were rinsed twice with PBS. After addition of 100 μl lysis buffer (25 mM Tris phosphate, pH 7.8, 2 mM dithiothreitol, 2 mM 1,2-diaminocyclohexane-N,N,N',N'-tetraacetic acid 10% glycerol, 1% Triton X-100), cells were scraped and transferred to a microcentrifuge tube placed on ice. Cell lysates were collected by vortexing for 10–15 sec and centrifugation at 12,000×g for 15 sec at 25 °C. The supernatant was assayed for both luciferase and β-galactosidase activities. The relative luciferase activity was calculated by dividing the luciferase activity by the β-galactosidase activity for each of the individual cell lysate samples.

2.9. Statistical Analysis

Unless otherwise indicated, data are represented as mean ± standard error with a sample size of three or more for each condition. A Student's t-test was performed to test for statistical significance in protein and albumin data with Microsoft Office Excel 2007. An Analysis of Variance (ANOVA) coupled with Tukey's post hoc analysis was performed to test statistical significance for HA quantification, macrophage cell proliferation, and TGF-β1 promoter activation assay with SPSS Statistics 20 (IBM). $p < 0.05$ was considered statistically significant.

3. RESULTS

3.1. Histological Analyses

AM tissue morphology and extracellular matrix (ECM) components were examined by histochemical staining of tissue sections. The thin, thick, and AMC tissue thickness for both fresh and cryopreserved samples ranged from 75–150 μm, 500–900 μm and 250–500 μm, respectively. H&E staining revealed that the structural morphology of CT-Thin (Fig. 1(B)) closely resembled that of F-Thin (Fig. 1(A)). Both tissues exhibited a thin basement membrane sandwiched between a simple epithelium and an avascular stroma that contained a cell-laden compact layer and a spongy layer. The chorion layer, consisting of an outer trophoblast layer and an inner somatic mesenchymal tissue, remained intact subjacent to the AM after cryopreservation in CT-AMC (Fig. 1(F)) and F-AMC (Fig. 1(E)). No apparent changes were noted in the density of ECM-collagen and sulfated proteoglycan after cryopreservation in any AM tissue when compared using Masson's Trichrome (Figs. 1(G)–(L)) and Safranin O staining (Figs. 1(M)–(R)). Collectively, these findings support the notion that cryopreservation did not cause notable changes in the histological properties of thin AM, thick AM, or AMC tissues as evidenced by the preservation of non-fibrillar collagen, proteoglycans, and glycoproteins.

3.2. Protein and Human Serum Albumin Analyses

The effects of cryopreservation on AM total protein and human serum albumin content were explored by BCA Protein Assay and Albumin ELISA, respectively. The total protein content of F-Thin and F-Thick tissues following extraction by 4M guanidine hydrochloride was significantly higher than that of CT-Thin and CT-Thick tissues (Table I, $p = 4.3\text{E-}05$ and $p = 3.2\text{E-}05$, respectively), but was not different between F-AMC and CT-AMC ($p = 0.42$). A similar, although not statistically significant trend was seen in serum albumin content where F-Thin and F-Thick albumin content appeared greater than in CT-Thin ($p = 0.10$) and CT-Thick ($p = 0.12$), and F-AMC and CT-AMC were similar ($p = 0.68$).

3.3. Biochemical Analyses of HA and HC-HA

Histochemistry with HABP was performed to determine whether cryopreservation affected the HA density of AM. HA staining was strongly positive in the AM stroma but weak in the amniotic epithelium for all fresh and cryopreserved AM (Figs. 2(A)–(F)). Additionally, HA was detected in the subjacent chorion of F-AMC (Figs. 2(E)) with a weaker staining for CT-AMC (Fig. 2(F)). Enzymatic treatment of histologic sections with *Streptomyces hyalurolyticus* HAase confirmed the specificity of HA staining (Figs. 2(G)–(L)).

To directly quantify the differences in ECM HA content, AMEs were prepared and analyzed using an HABP assay. Although all cryopreserved samples appeared to show an increased HA/total protein ratio compared to their fresh counterparts (Fig. 3), the results only reached significance in the CT-Thin and CT-Thick samples ($p = 0.011$ and $p = 1.4\text{E-}12$, respectively). CT-Thin also had a significantly larger HA/total protein ratio than CT-AMC ($p = 0.0011$), likely due to the chorion contributing to an increase in total protein while appearing to have comparatively little HA histochemistry (Fig. 2(F)).

The molecular weight (MW) of HA has been tied to different biological outcomes *in vivo*.[29] To further determine

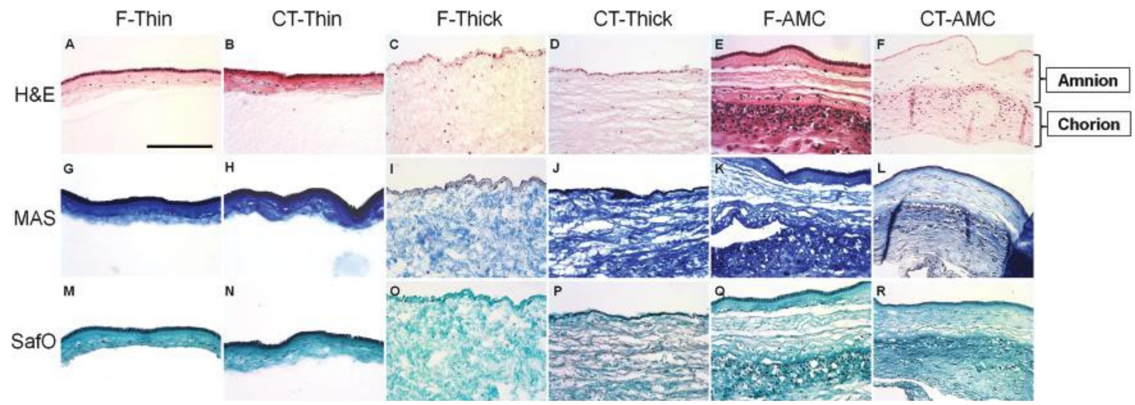

Fig. 1. Histological analyses. Six different types of tissues were prepared: fresh and cryopreserved AM (F-Thin, CT-Thin, F-Thick, CT-Thick), and fresh and cryopreserved amniochorion (F-AMC, CT-AMC). Samples were subsequently fixed in formalin, embedded in paraffin for sectioning, and stained with hematoxylin and eosin (H&E), Masson's Trichrome (MAS) or Safranin O (SafO) to visualize tissue morphology, collagen, and sulfated proteoglycans, respectively. The ECM structural morphology (H&E), proteoglycan (SafO) and collagen (MAS) density did not appear altered by the cryopreservation process. Bar = 200 μm represented by A.

Table I. Protein and human serum albumin contents. Samples were homogenized, extracted with 4M guanidine hydrochloride, dialyzed against PBS, and analyzed for protein and albumin content in triplicate. The content of protein and human serum albumin was normalized to the tissue weight; $n = 3$.

Samples	Protein/ weight (mg/g)	*p*-value	Albumin/ weight (mg/g)	*p*-value	Albumin/ protein ratio (mg/mg)
F-Thin	4.76 ± 0.079	4.3E-05	0.069 ± 0.023	0.10	0.015
CT-Thin	1.56 ± 0.11		0.0017 ± 0.0003		0.0011
F-Thick	5.91 ± 0.087	3.2E-05	0.94 ± 0.34	0.12	0.16
CT-Thick	1.18 ± 0.14		0.037 ± 0.018		0.031
F-AMC	13.6 ± 1.4	0.42	0.30 ± 0.10	0.68	0.022
CT-AMC	12.1 ± 0.48		0.35 ± 0.04		0.029

the size distribution of HA in AM extracts, we used agarose gel electrophoresis followed by Stains-all dye as previously described.[26] HA appeared as a bluish stain in all AMEs and the staining was shown to be specific for HA by the disappearance of the HMW HA fraction with HAase digestion (Fig. 4, HAase (+), Lanes 2, 5 and 6). Cryopreservation appeared to maintain the HA integrity, as no difference in molecular size distribution was observed between fresh and cryopreserved samples. HA from Thick AM samples (Fig. 4, HAase(−), Lanes 5 and 6) exhibited the same HMW distribution as the Healon® control (Fig. 4, HAase(−), Lane 2) in the range of 1000 to 6000 kDa, indicating that thick tissue preferentially contained HMW HA compared to Thin and AMC tissues. Unlike Healon®, a HMW band was detected in the loading well from CT-Thin and CT-Thick and their fresh counterparts (Fig. 4, HAase(−), Lane 3-6) which was abolished following HAase digestion (Fig. 4, HAase(+), Lane 3-6), suggesting the presence of a HMW HA species in AMEs that was larger than that of Healon®. In contrast, no HMW band from cryopreserved and fresh AMC remained in the loading wells.

The abundance of HMW HA in AMEs was consistent with the constitutive production of heavy chain-hyaluronic acid (HC-HA) complex observed in AM tissue[30] where the heavy chains (HC) of the inter-α-inhibitor (IαI) protein were transferred and covalently linked to HA forming a very HMW complex. To determine if the heavy chains (HCs) of IαI are associated with the HA in AMEs, samples were subjected to HAase to digest HA into small

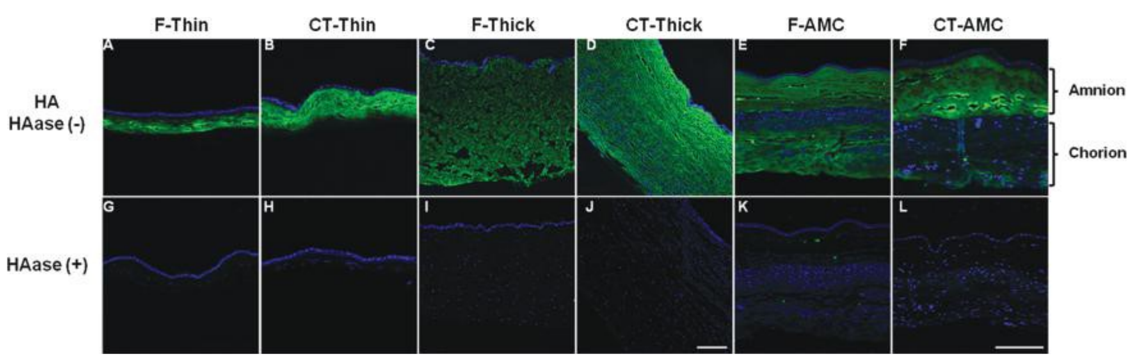

Fig. 2. HA histochemistry of fresh and cryopreserved tissues. De-paraffinized sections of different tissues were labeled with biotinylated HABP with or without HAase digestion. HA distribution throughout the AM tissue was retained following cryopreservation in all tissue samples. Due to differences in tissue sizes, the thick tissue images were taken at a lower magnification in order to fully visualize the entire section. Bar = 200 μm for all images.

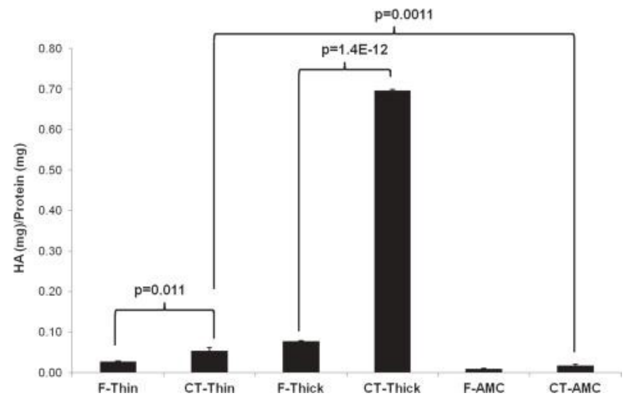

Fig. 3. Relative HA content. AMEs quantified for HA using an HA Testing Kit and for proteins using BCA assay. The HA to total protein ratio was significantly higher for cryopreserved samples compared to their fresh counterparts for both the Thin and Thick tissues ($p = 0.011$ and $p = 1.4$E-12, respectively); $n = 3$.

fragments before Western blot analysis with an anti-HC1 antibody. As expected, IαI purified from human plasma yielded a major band at ~250 kDa (Fig. 5, Lane 2) and treatment of IαI with 50 mM NaOH cleaved the ester bonds linking the HCs to IαI to yield 75 kDa HC1 fragments (Fig. 5, Lane 3).[31–35] The HMW band on the top of the gel of all tissues except those containing chorion (F-AMC and CT-AMC) was partially cleaved following HAase digestion to yield an increase in the intensity of the 75 kDa HC1 fragment (Fig. 5, Lanes 4–11) indicating that the HC-HA complex is present in AM tissues. Both CT-Thin and CT-Thick samples appeared to retain the HC-HA complex following the cryopreservation process.

3.4. Biological Analyses

AM's anti-inflammatory activity can be demonstrated by the suppression of viability and proliferation of macrophages by both AM tissue[36] and AME.[25] To further explore the effect of cryopreservation on cell viability, RAW264.7 macrophages were seeded at the same density directly on the stromal surface of both CT-Thin and F-Thin tissues. A high proportion of resting macrophages on plastic culture dishes had an oval morphology evenly distributed with some scattered spindle cells. When seeded on cryopreserved AM tissue, the cells aggregated and became rounded (Figs. 6I, (B)) more than the fresh tissue samples at 48 h (Figs. 6(I), (A)). The majority of cells on both fresh and cryopreserved AM tissue were viable and the presence and distribution of dead cells across the surface was similar displaying shrunken and condensed morphology in both cryopreserved and fresh AM tissues (Figs. 6(I), (C) and (D)).

Cell proliferation was measured by BrdU labeling following RAW264.7 treatment with 100 μg/ml of either fresh or cryopreserved AME (Fig. 6(II)). Compared to cells in the PBS vehicle control (CTL), cells treated with both fresh and cryopreserved AME samples significantly inhibited RAW264.7 macrophage proliferation ($p = 8.6$E-5 and $p = 1.8$E-5, respectively). There was no significant difference in cell proliferation between the fresh and cryopreserved AM samples ($p = 0.22$).

The role of TGF-β1 signaling in fibroblast-mediated scar formation has been well documented.[37] In animal wound models, inhibiting TGF-β signaling in local fibroblasts decreases the extent of scar formation while adding exogenous TGF-β enhances fibrosis and scar formation at

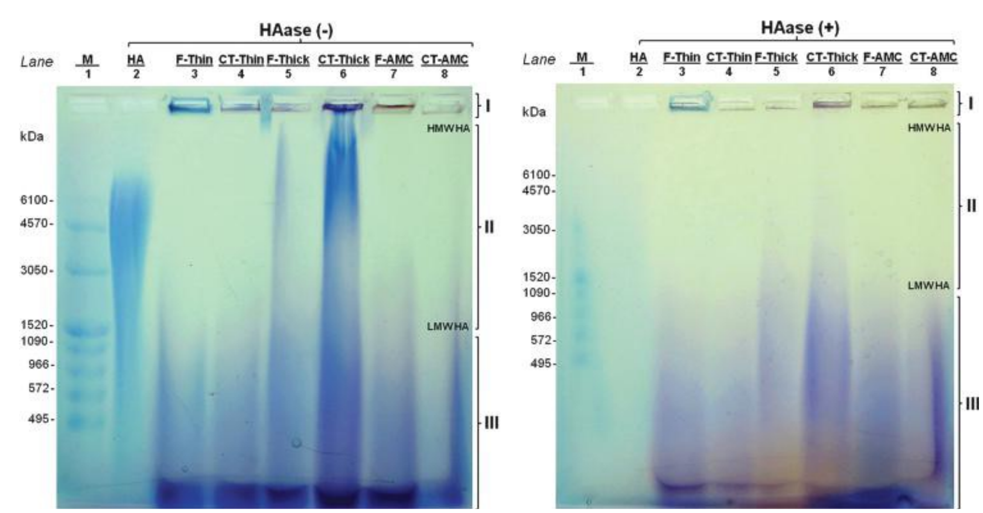

Fig. 4. HA molecular weight analysis. AM tissue extracts were loaded at 15 μg HA per lane with or without pre-digestion with HAase for 1 h at 37 °C to determine the HA size. The MW of Select-HA HiLadder (M, Lane 1) was marked to the left and HMW HA control based on Healon® (Lane 2) is included as a comparison. The HMW HA species retained in the loading well is labeled I and other HMW HA (1000–6000 kDa) and LMW species (< 1000 kDa) are labeled II and III, respectively. The Thin and Thick tissues for both fresh and cryopreserved samples revealed HMW HA retained in the loading well but, only the Thick tissue for both fresh and cryopreserved contained HMW HA within the gel.

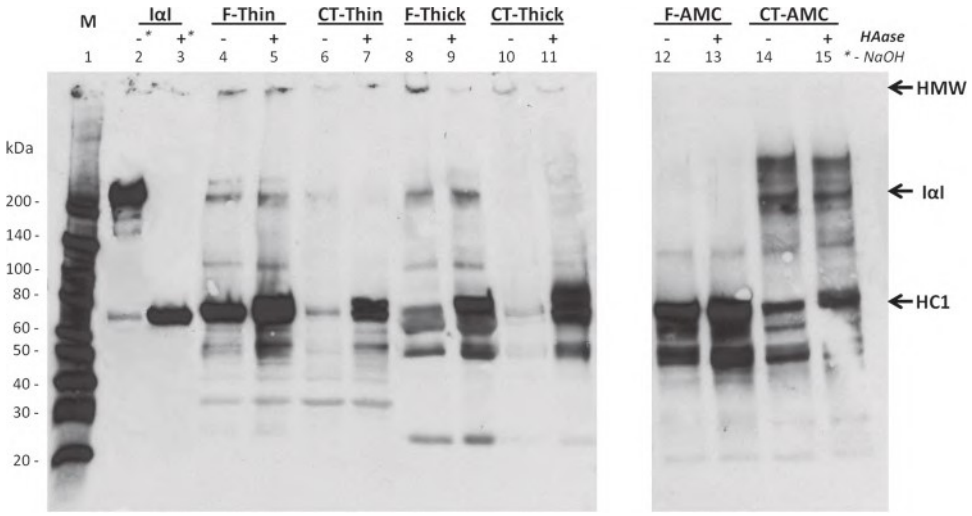

Fig. 5. Western blot detection of HC-HA complex. Tissue extracts by 4 M guanidine hydrochloride at 20 μg protein/well were treated with and without HAase before Western blot analysis using an anti-HC1 antibody, and compared to the control, i.e., IαI, purified from human plasma. The HMW band on the top of the gel of all tissues except those containing chorion (F-AMC and CT-AMC) was partially cleaved following HAase digestion to yield an increase in the intensity of the 75 kDa HC1 fragment (Lanes 4–11) indicating that the HC-HA complex is present AM tissues.

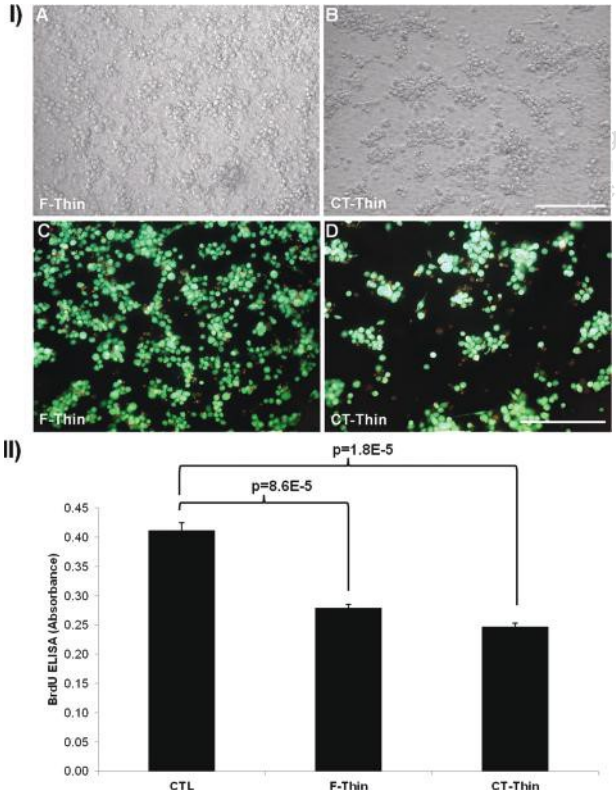

Fig. 6. Macrophage viability and proliferation assay. (I) Phase images reveal attachment of RAW264.7 cells on fresh (A) and cryopreserved thin AM tissue (B). LIVE/DEAD staining demonstrates the majority of the cells on fresh and cryopreserved AM remain viable (green fluorescence) with only a few dead (red fluorescence) macrophage cells after 48 h culture. Scale bar= 100 μm. (II) Proliferation of PBS vehicle control (CTL) RAW264.7 macrophage cells were significantly inhibited when treated with F-Thin ($p = 8.6$E-5) and CT-Thin ($p = 1.8$E-5) extracts at 100 μg/mL protein and BRDU labeling for 1 h; $n = 3$.

the wound site.[37] We have previously demonstrated the down-regulation of TGF-β1 signaling in human corneal fibroblasts by both cryopreserved AM tissue[38] and HC-HA complex purified from cryopreserved AME.[35] However, a comparison of the ability of fresh and cryopreserved AME to modify TGF-β signaling has not previously been done. To better understand the effect of cryopreservation on modulating amnion-mediated TGF-β signaling, we measured the TGF-β1 promoter activity in cultured human corneal fibroblasts treated with PBS vehicle control (CTL)

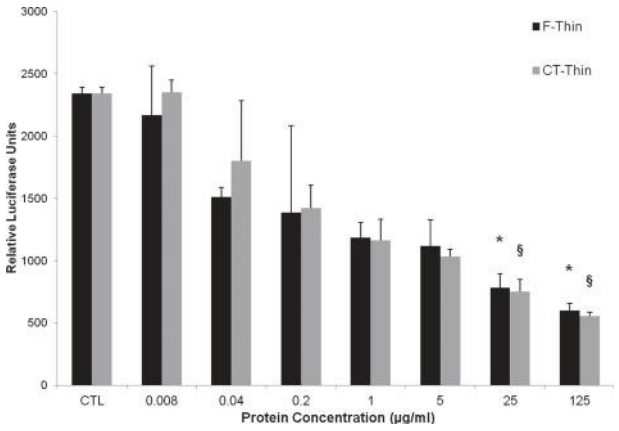

Fig. 7. Inhibition of TGF-β1 promoter activation by fresh and cryopreserved AME. A series of protein concentration (0.008–125 μg/ml) from F-Thin and CT-Thin were used to analyze TGF-β1 promoter activation. Cell lysates were assayed for both luciferase and β-galactosidase measurement, and data is expressed as relative luciferase/β-galactosidase units. $n = 3$ for all experiments. There was a significant inhibition of TGF-β1 at the two highest doses analyzed in comparison to the PBS vehicle control (CTL), and there was no significant difference between fresh and cryopreserved samples. $* = p < 0.05$ compared to CTL, § = $p < 0.05$ compared to CTL.

and either fresh or cryopreserved AME in a series of protein concentration ranging from 0.008–125 μg/ml. Both fresh and cryopreserved AME (Fig. 7) exhibited a significant inhibition of the TGF-β1 promoter activity at the two highest doses, 25 μg/ml ($p = 0.011$ and $p = 0.088$ for fresh and cryopreserved, respectively) and 125 μg/ml ($p = 0.0028$ and $p = 0.020$ for fresh and cryopreserved, respectively). However, no difference in TGF-β1 suppression was observed between fresh and cryopreserved AME treatment at either 25 or 125 μg/ml ($p = 1.0$ and $p = 1.0$, respectively), indicating the cryopreservation process did not alter the ability of AM tissue to decrease TGF-β1 activity.

4. DISCUSSION

The use of fresh AM tissue for clinical applications is both impractical and poses a serious risk of disease transmission.[20,21] Tissue preservation and storage are essential for maintaining the biological therapeutic actions of the fresh material and are critical to the successful commercialization of AM tissues for clinical use. While multiple AM preservation methods exist (including dehydration, lyophilization, chemical cross-linking, and cryopreservation), these processing methods all have variable effects on preserving the native form of AM tissue and can dramatically alter the type of host response elicited to the material when utilized as templates for tissue regeneration.[22] Cryopreservation allows for the quarantine of donor tissue, enabling additional precautions to prevent the risk of introducing and transmitting communicable diseases the AM may harbor.[20,21,39] The present comparative study demonstrates that cryopreserved AM maintained the native tissue integrity of fresh AM as well as preserved native biological components crucial for the therapeutic efficacy of the tissue. Together, these findings demonstrate that cryopreservation preserves the histological structure, the extracellular matrix composition and biologic activity of native AM.

Cryopreserved AM tissue was similar in morphology, collagen, and glycoaminoglycan density and distribution in comparison to the fresh AM tissue (Fig. 1). These findings agree with those previously reported[40] where cryopreserved AM retained basement membrane components after 2 years of storage at -80 °C. Previous studies have revealed that AM's wound healing potential is mediated by the complex assembly of cytokines, chemokines, and growth factors.[1,41–44] Given this, the retention of these proteins is an essential feature of any preservation method. Cryopreservation did not remove the essential biochemical component HA, which has been implicated in contributing to both the anti-inflammatory and anti-scarring properties of AM.[25,35] Both cryopreserved and fresh tissues contained HA detected by histochemistry and HABP quantification (Figs. 2 and 3) indicating there was retention of this key biological molecule after cryopreservation, which may contribute significantly to the clinical biological action of the tissue. Cryopreservation reduced the total protein and human serum albumin content in both thin and thick AM tissues when compared to their fresh counterparts (Table I). We speculate that this difference resulted from the gentle rinsing step with PBS and the freezing step employed by the cryopreservation process to remove the residual blood contaminants from procurement. These steps were not employed for fresh tissues. Consequently, we noted a significantly higher HA to total protein ratio for CT-Thin and CT-Thick samples when compared to their fresh counterparts (Fig. 3).

Further biochemical analysis established the presence of HMW HA in both fresh and cryopreserved Thick and Thin tissues (Fig. 4). Unlike low molecular weight (LMW) HA, which has been shown to be pro-inflammatory, HMW HA exerts anti-inflammatory properties[45] and therefore is more relevant to therapeutic applications. Additionally, we have reported that HMW HA in AM existed as a HC-HA complex formed by a covalent bond between HA and HC1 of inter-α-inhibitor[30,35] (IαI) and that this HC-HA complex exerts more potent anti-inflammatory and anti-scarring effects than HMW HA alone.[35] The HC-HA complex was detected by Western Blot in both cryopreserved and fresh AM tissues, indicating that cryopreservation does not disrupt this vital biological component.

The effects of AM on inflammatory-cell viability and proliferation[25] can be replicated *in vitro* with cryopreserved AM tissue,[36] AME[25] and the HC-HA complex purified from AME.[30,35] These actions, however, have never been compared with fresh AM tissues or extracts. Herein, we confirmed that macrophages seeded on both fresh and cryopreserved AM display viable cell numbers (Fig. 6). Furthermore, when AME from cryopreserved AM is added at the same protein amount as fresh AM, it is just as effective in suppressing the proliferation of RAW264.7 macrophages (Fig. 7). Also, a direct anti-scarring action by AM seen clinically has been attributed to the suppression of TGF-β1 signaling at the transcriptional level of fibroblast cells derived from ocular tissues treated with AM.[38,46–48] Cryopreserved AM suppresses TGF-β signaling by downregulating TGFβRII[38] and preventing phosphorylation of Smad2/3 and its subsequent binding to Smad4 to form heteromeric Smad complexes that would enter the nucleus to initiate TGF-β gene transcription.[28] Both CT-Thin and F-Thin AME at 25 μg/ml and 125 μg/ml protein were able to significantly inhibit TGF-β1 promoter activity in human corneal fibroblasts (Fig. 7) with no significant differences exhibited as a result of the cryopreservation process. Altogether, the similar macrophage morphology and viability, suppression of macrophage proliferation, and reduction of TGF-β1 promoter activity by both fresh and processed tissues further

indicate that cryopreservation maintains the effectiveness of the bioactive components of AM.

Overall, this study found no distinguishable differences between the histological and biochemical features of fresh and cryopreserved AM tissues. Although total protein and albumin contents were reduced after cryopreservation, the levels of both HA and HC-HA complex were maintained in cryopreserved tissues. Consequently, cryopreserved AM extracts were as effective as fresh AM extracts in suppressing RAW264.7 macrophage proliferation and down-regulating TGF-β1 signaling in human corneal fibroblasts.

5. CONCLUSION

Collectively, the data support cryopreserved AM is comparable to fresh AM with regards to structural integrity and retention of key biochemical components essential for the biological functions, indicating that cryopreservation offers a safe and effective means of preserving AM tissue.

Disclosure Statement

Scheffer C. G. Tseng and his family are more than 5% shareholders of TissueTech, Inc. TissueTech, Inc. and its Subsidiaries (Bio-Tissue, Inc. and Amniox Medical) own US Patents Nos. 6152142, 6326019, and *PCT/US2010/046675* on the method of preparation and clinical uses of human amniotic membrane with the CryoTek™ method distributed by Bio-Tissue, Inc. and Amniox Medical. Scheffer C. G. Tseng, E. K. Tan, M. Mahabole and H. He are employees of TissueTech, Inc. J. O'Connell is an employee and shareholder of Amniox Medical. T. C. McDevitt was a former consultant for Amniox Medical. M. T. Cooke and C. Mandrycky have no financial conflict.

Acknowledgment: This research was supported by a Venture Lab Grant #398 from the Georgia Research Alliance, Atlanta, GA, and a research grant from TissueTech, Inc., Miami, FL. The authors gratefully acknowledge the technical assistance provided by Suzhen Zhang from TissueTech, Inc., Miami, FL.

References and Notes

1. S. C. Tseng, E. M. Espana, T. Kawakita, M. A. Di Pascuale, W. Li, H. He, T. S. Liu, T. H. Cho, Y. Y. Gao, L. K. Yeh, and C. Y. Liu, How does amniotic membrane work?. *Ocul. Surf.* 2, 177 **(2004)**.
2. J. Liu, H. Sheha, Y. Fu, L. Liang, and S. C. Tseng, Update on amniotic membrane transplantation. *Expert. Rev. Ophthalmol.* 5, 645 **(2010)**.
3. J. W. Davis, Skin transplantation with a review of 550 cases at the Johns Hopkins Hospital. *Johns. Hopkins Med. J.* 15, 307 **(1910)**.
4. J. S. Gruss and D. W. Jirsch, Human amniotic membrane: A versatile wound dressing. *Can. Med. Assoc. J.* 118, 1237 **(1978)**.
5. W. P. Faulk, R. Matthews, P. J. Stevens, J. P. Bennett, H. Burgos, and B. L. Hsi, Human amnion as an adjunct in wound healing. *Lancet* 1, 1156 **(1980)**.
6. W. J. Peters, Biological dressings in burns—A review. *Ann. Plast. Surg.* 4, 133 **(1980)**.
7. M. R. Kesting, K. D. Wolff, B. Hohlweg-Majert, and L. Steinstraesser, The role of allogenic amniotic membrane in burn treatment. *J. Burn. Care Res.* 29, 907 **(2008)**.
8. J. P. Bennett, R. Matthews, and W. P. Faulk, Treatment of chronic ulceration of the legs with human amnion. *Lancet* 1, 1153 **(1980)**.
9. H. Swift, Amnion for leg ulcers. *Lancet* 1, 1366 **(1980)**.
10. H. S. Dua, J. A. Gomes, A. J. King, and V. S. Maharajan, The amniotic membrane in ophthalmology. *Surv. Ophthalmol.* 49, 51 **(2004)**.
11. C. S. Bouchard and T. John, Amniotic membrane transplantation in the management of severe ocular surface disease: Indications and outcomes. *Ocul. Surf.* 2, 201 **(2004)**.
12. D. Meller, M. Pauklin, H. Thomasen, H. Westekemper, and K. P. Steuhl, Amniotic membrane transplantation in the human eye. *Dtsch. Arztebl. Int.* 108, 243 **(2011)**.
13. B. A. Mast, R. F. Diegelmann, T. M. Krummel, and I. K. Cohen, Scarless wound healing in the mammalian fetus. *Surg. Gynecol. Obstet.* 174, 441 **(1992)**.
14. N. S. Adzick and H. P. Lorenz, Cells, matrix, growth factors, and the surgeon. The biology of scarless fetal wound repair. *Ann. Surg.* 220, 10 **(1994)**.
15. F. Demirkan, N. Colakoglu, O. Herek, and G. Erkula, The use of amniotic membrane in flexor tendon repair: An experimental model. *Arch. Orthop. Trauma Surg.* 122, 396 **(2002)**.
16. J. J. Yang, E. C. Jang, W. S. Song, J. S. Lee, M. K. Kim, and S. H. Chang, The effect of amniotic membrane transplantation on tendon-healing in a rabbit achilles tendon model. *Tissue Engineering and Regenerative Medicine* 7, 323 **(2010)**.
17. J. Mohammad, J. Shenaq, E. Rabinovsky, and S. Shenaq, Modulation of peripheral nerve regeneration: A tissue-engineering approach. The role of amnion tube nerve conduit across a 1-centimeter nerve gap. *Plast Reconstr. Surg.* 105, 660 **(2000)**.
18. S. S. Kim, S. K. Sohn, K. Y. Lee, M. J. Lee, M. S. Roh, and C. H. Kim, Use of human amniotic membrane wrap in reducing perineural adhesions in a rabbit model of ulnar nerve neurorrhaphy. *J. Hand Surg. Eur. Vol.* 35, 214 **(2010)**.
19. H. Meng, M. Li, F. You, J. Du, and Z. Luo, Assessment of processed human amniotic membrane as a protective barrier in rat model of sciatic nerve injury. *Neurosci. Lett.* 496, 48 **(2011)**.
20. T. Maral, H. Borman, H. Arslan, B. Demirhan, G. Akinbingol, and M. Haberal, Effectiveness of human amnion preserved long-term in glycerol as a temporary biological dressing. *Burns* 25, 625 **(1999)**.
21. P. J. Adds, C. J. Hunt, and J. K. Dart, Amniotic membrane grafts, "fresh" or frozen? A clinical and in vitro comparison. *Br. J. Ophthalmol.* 85, 905 **(2001)**.
22. S. F. Badylak, Regenerative medicine and developmental biology: The role of the extracellular matrix. *Anat. Rec. B New Anat.* 287, 36 **(2005)**.
23. A. M. Blom, M. Morgelin, M. Oyen, J. Jarvet, and E. Fries, Structural characterization of inter-alpha-inhibitor. Evidence for an extended shape. *J. Biol. Chem.* 274, 298 **(1999)**.
24. M. Muramatu, S. Mori, Y. Matsuzawa, Y. Horiguchi, Y. Nakanishi, and M. Tanaka, Purification and characterization of urinary trypsin inhibitor, UTI68, from normal human urine, and its cleavage by human uropepsin. *J. Biochem.* 88, 1317 **(1980)**.
25. H. He, W. Li, S. Y. Chen, S. Zhang, Y. T. Chen, Y. Hayashida, Y. T. Zhu, and S. C. Tseng, Suppression of activation and induction of apoptosis in RAW264.7 cells by amniotic membrane extract. *Invest. Ophthalmol. Vis. Sci.* 49, 4468 **(2008)**.
26. H. G. Lee and M. K. Cowman, An agarose gel electrophoretic method for analysis of hyaluronan molecular weight distribution. *Anal. Biochem.* 219, 278 **(1994)**.
27. W. Li, H. He, C. L. Kuo, Y. Gao, T. Kawakita, and S. C. Tseng, Basement membrane dissolution and reassembly by limbal corneal epithelial cells expanded on amniotic membrane. *Invest. Ophthalmol. Vis. Sci.* 47, 2381 **(2006)**.

28. T. Kawakita, E. M. Espana, H. He, A. Hornia, L. K. Yeh, J. Ouang, C. Y. Liu, and S. C. Tseng, Keratocan expression of murine keratocytes is maintained on amniotic membrane by downregulating TGF-beta signaling. *J. Biol. Chem.* 280, 27085 **(2005)**.

29. H. Morrison, L. S. Sherman, J. Legg, F. Banine, C. Isacke, C. A. Haipek, D. H. Gutmann, H. Ponta, and P. Herrlich, The NF2 tumor suppressor gene product, merlin, mediates contact inhibition of growth through interactions with CD44. *Genes Dev.* 15, 968 **(2001)**.

30. S. Zhang, H. He, A. J. Day, and S. C. Tseng, Constitutive expression of inter-alpha-inhibitor (IalphaI) family proteins and tumor necrosis factor-stimulated gene-6 (TSG-6) by human amniotic membrane epithelial and stromal cells supporting formation of the heavy chain-hyaluronan (HC-HA) complex. *J. Biol. Chem.* 287, 12433 **(2012)**.

31. M. Yoneda, S. Suzuki, and K. Kimata, Hyaluronic acid associated with the surfaces of cultured fibroblasts is linked to a serum-derived 85-kDa protein. *J. Biol. Chem.* 265, 5247 **(1990)**.

32. J. J. Enghild, G. Salvesen, S. A. Hefta, I. B. Thogersen, S. Rutherfurd, and S. V. Pizzo, Chondroitin 4-sulfate covalently cross-links the chains of the human blood protein pre-alpha-inhibitor. *J. Biol. Chem.* 266, 747 **(1991)**.

33. T. E. Jessen, L. Odum, and A. H. Johnsen, In vivo binding of human inter-alpha-trypsin inhibitor free heavy chains to hyaluronic acid. *Biol. Chem. Hoppe Seyler* 375, 521 **(1994)**.

34. M. Zhao, M. Yoneda, Y. Ohashi, S. Kurono, H. Iwata, Y. Ohnuki, and K. Kimata, Evidence for the covalent binding of SHAP, heavy chains of inter-alpha-trypsin inhibitor, to hyaluronan. *J. Biol. Chem.* 270, 26657 **(1995)**.

35. H. He, W. Li, D. Y. Tseng, S. Zhang, S. Y. Chen, A. J. Day, and S. C. Tseng, Biochemical Characterization and Function of Complexes Formed by Hyaluronan and the Heavy Chains of Inter-a-inhibitor (HC · HA) Purified from Extracts of Human Amniotic Membrane. *J. Biol. Chem.* 284, 20136 **(2009)**.

36. W. Li, H. He, T. Kawakita, E. M. Espana, and S. C. G. Tseng, Amniotic membrane induces apoptosis of interferon-gamma activited macrophages in vitro. *Exp. Eye Res.* 82, 282 **(2006)**.

37. M. W. Ferguson, Wound healing–scar wars. *Ulster Med. J.* 67, 37 **(1998)**.

38. S. C. Tseng, D. Q. Li, and X. Ma, Suppression of transforming growth factor-beta isoforms, TGF-beta receptor type II, and myofibroblast differentiation in cultured human corneal and limbal fibroblasts by amniotic membrane matrix. *J. Cell Physiol.* 179, 325 **(1999)**.

39. F. B. Marangon, E. C. Alfonso, D. Miller, N. M. REmonda, M. S. Muallem, and S. C. Tseng, Incidence of microbial infection after amniotic membrane transplantation. *Cornea* 23, 264 **(2004)**.

40. H. Thomasen, M. Pauklin, B. Noelle, G. Geerling, J. Vetter, P. Steven, K. P. Steuhl, and D. Meller, The effect of long-term storage on the biological and histological properties of cryopreserved amniotic membrane. *Curr. Eye Res.* 36, 247 **(2011)**.

41. N. Koizumi, T. Inatomi, C. Sotozono, N. J. Fullwood, A. J. Quantock, and S. Kinoshita, Growth factor mRNA and protein in preserved human amniotic membrane. *Curr. Eye Res.* 20, 173 **(2000)**.

42. A. Hopkinson, R. S. McIntosh, P. J. Tighe, D. K. James, and H. S. Dua, Amniotic membrane for ocular surface reconstruction: Donor variations and the effect of handling on TGF-beta content. *Invest. Ophthalmol. Vis. Sci.* 47, 4316 **(2006)**.

43. S. Wolbank, F. Hildner, H. Redl, G. M. van, C. Gabriel, and S. Hennerbichler, Impact of human amniotic membrane preparation on release of angiogenic factors. *J. Tissue Eng. Regen. Med.* 3, 651 **(2009)**.

44. U. Schulze, U. Hampel, S. Sel, T. W. Goecke, V. Thale, F. Garreis, and F. Paulsen, Fresh and cryopreserved amniotic membrane secrete the trefoil factor family peptide 3 that is well known to promote wound healing. *Histochem. Cell Biol.* **(2012)**.

45. C. M. McKee, M. B. Penno, M. Cowman, M. D. Burdick, R. M. Strieter, C. Bao, and P. W. Noble, Hyaluronan (HA) fragments induce chemokine gene expression in alveolar macrophages. The role of HA size and CD44. *J. Clin. Invest.* 98, 2403 **(1996)**.

46. S. B. Lee, D. Q. Li, D. T. Tan, D. C. Meller, and S. C. Tseng, Suppression of TGF-beta signaling in both normal conjunctival fibroblasts and pterygial body fibroblasts by amniotic membrane. *Curr. Eye Res.* 20, 325 **(2000)**.

47. G. Gabbiani, The myofibroblast in wound healing and fibrocontractive diseases. *J. Pathol.* 200, 500 **(2003)**.

48. W. Li, H. He, Y. T. Chen, Y. Hayashida, and S. C. Tseng, Reversal of myofibroblasts by amniotic membrane stromal extract. *J. Cell Physiol.* 215, 657 **(2008)**.

Received: 27 February 2014. Accepted: 26 March 2014.